

An iteration approach for multiple notch problem based on complex variable boundary integral equation

Y. Z. Chen*

Division of Engineering Mechanics, Jiangsu University, Zhenjiang, Jiangsu, 212013, P.R. China

(Received November 22, 2011, Revised January 20, 2012, Accepted January 28, 2012)

Abstract. This paper provides an iteration approach for the solution of multiple notch problem, which is based on the complex variable boundary integral equation (CVBIE). The contours of notches are applied by some loadings. The source points are assumed on the boundary of individual notch and the displacements along the boundaries become unknowns to be investigated. After discretization of the BIE, many influence matrices are obtained. One does not need to assemble many influence matrices into a larger matrix. This will considerably reduce the work in the program. The displacements along the many boundaries can be obtained from an iteration. There is no limitation for the configuration of notches. Several numerical examples are provided to prove the efficiency of the suggested approach.

Keywords: boundary integral equation; multiple notches; stress concentration factors; iteration

1. Introduction

The boundary integral equation methods (BIE) were initiated by many pioneer researchers (Rizzo 1967, Cruse 1969, Jaswon and Symm 1977, Brebbia *et al.* 1984, Hong and Chen 1988, Cheng and Cheng 2005). Generally, it is difficult or impossible to find a solution in a closed form for an arbitrary geometry of boundary, if one directly uses the BIE. Therefore, the boundary element method (BEM) was suggested to solve BIE numerically. The BEM distinguishes itself as a boundary method, meaning that the numerical discretization is conducted at reduced spatial dimension (Cheng and Cheng 2005). Particularly, it is difficult to model elasticity problem for the infinite region by using the finite element method. However, BIE can model the elasticity problem for the infinite region without any difficulty.

Many researchers studied the stress concentration problems for multiple circular holes and elliptic notches (Muskhelishvili 1963, Savin 1961, Nisitani 1978, Isida and Igawa 1991, Denda and Kosaka 1997, Tsukrov and Kachanov 1997, Ting *et al.* 1999a, b, c, Wang *et al.* 2003). A closed form solution for a single elliptic notch was obtained in an earlier time (Muskhelishvili 1963). Many results for stress concentration were collected in (Savin 1961). For a single circular hole in an infinite domain subjected to the arbitrary tractions across the circle boundary, an analytical solution was derived. The multiple circular hole problem was solved by an alternative method (Ting *et al.*

*Corresponding author, Professor, E-mail: chens@ujs.edu.cn

1999a, b). Multiple circular hole problem was solved by a complex variable boundary integral equation method combined with series expansion technique (Wang *et al.* 2003). It is seen from those references that the studied problems were mainly limited to the cases of the circular or the elliptic contour.

Recently, a null-field approach for the multi-inclusion problem under antiplane shears was suggested (Chen and Wu 2007). In addition, the torsional rigidity of a circular bar with multiple circular inclusions was investigated, which is based on the null-field integral approach (Chen and Lee 2009). Solution of periodic notch problems in an infinite plate was presented, where a BIE in conjunction with remainder estimation technique was suggested (Chen 2011). A hypersingular boundary integral equation was developed to solve a plane elasticity problem of finite region (Zhang and Zhang 2008).

By using the finite element method, the through-thickness variations of stress concentration factors along the wall of elliptic holes in finite thickness plates of isotropic materials subjected to remote tensile stress were studied (She and Guo 2007). Three-dimensional stress fields near notches and cracks were studied (She *et al.* 2008). The strength of the structures with stress gradient usually shows strong three-dimensional (3D) effects even under in-plane loading. The elastic stress and strain fields in a plate of finite thickness containing an elliptical hole are investigated using the 3D finite element method (Yang 2009). The elastic stress and strain fields of finite thickness large plate containing a hole are systematically investigated using 3D finite element method (Yang *et al.* 2008). The variation of the stress and strain concentration factors along the thickness are studied in detail.

A boundary element method was developed to solve the doubly periodic inclusion problem in an infinite plate (Dong and Lee 2006). The effective elastic modulus was evaluated. In the formulation, if the inclusion is very soft the inclusion problem will reduce to the hole problem. By using the boundary integral equation method, the effective elastic properties of doubly periodic array of inclusions of various shapes by the boundary element method were investigated (Dong 2006).

In an earlier year, a boundary element method was developed to analyze the stress concentration problems of multiple elliptical holes in an infinite domain (Ting *et al.* 1999c). In the formulation, the tractions on the hole contours were chosen as an iteration parameter. In the case of the elliptical holes, many computed results for stress concentration factor were presented.

This paper provides an iteration approach for the solution of multiple notch problem, which is based on complex variable boundary integral equation (CVBIE). It is assumed that the contours of notches are applied by some loadings. In the formulation, the source points are assumed on the boundary of individual notch. The displacements along the boundaries become unknowns to be investigated. After discretization of the BIE, many influence matrices are obtained. In the suggested iteration approach, one does not need to assemble many influence matrices into a larger matrix. This will considerably reduce the work in the program. In addition, the displacements along the many boundaries can be obtained from an iteration. From the computed results for displacements along boundaries, the hoop stress around notches can be finally determined. There is no limitation for the configuration of notches. Several numerical examples including five elliptic notches in series and two square notches are provided to prove the efficiency of the suggested approach. Stress intensity factors (SIFs) are evaluated in all numerical examples.

2. Analysis

2.1 Boundary integral equation for multiple notch problem

Recently, a boundary integral equation for an exterior region using complex variable (CVBIE) was suggested (Chen and Lin 2010), which is equivalent to the formulation based on real variable (Brebbia *et al.* 1984, Cheng and Cheng 2005, Chen *et al.* 1995). Comparing the CVBIE with that in real variable, the suggested CVBIE is more informative because the behavior of involved kernels can easily be recognized from their explicit form (see below Eqs. (1) to (4)). Some relevant formulations for BIEs based on complex variable can be referred to (Chen *et al.* 2002, Chen and Chen 2000, Kolte *et al.* 1996, Linkov 2002, Mogilevskaya and Linkov 1998, Mogilevskaya 2000).

The suggested CVBIE for exterior region takes the following form (Chen and Lin 2010) (Fig. 1)

$$\begin{aligned} & \frac{U(t_o)}{2} - B_1 i \int_{\Gamma} \left(\frac{\kappa-1}{t-t_o} U(t) dt - L_1(t, t_o) U(t) dt + L_2(t, t_o) \overline{U(t)} dt \right) \\ & = -B_2 i \int_{\Gamma} \left(2\kappa \ln|t-t_o| Q(t) dt + \frac{t-t_o}{\bar{t}-\bar{t}_o} \overline{Q(t)} d\bar{t} \right), \quad (t_o \in \Gamma) \end{aligned} \tag{1}$$

where Γ denotes the boundary of notch, and

$$U(t) = u(t) + iv(t), \quad Q(t) = \sigma_N(t) + i\sigma_{NT}(t), \quad (t \in \Gamma) \tag{2}$$

$$B_1 = \frac{1}{2\pi(\kappa+1)}, \quad B_2 = \frac{1}{4\pi G(\kappa+1)} \tag{3}$$

$$L_1(t, \tau) = -\frac{d}{dt} \left\{ \ln \frac{t-\tau}{\bar{t}-\bar{\tau}} \right\} = -\frac{1}{t-\tau} + \frac{1}{\bar{t}-\bar{\tau}} \frac{d\bar{t}}{dt}$$

$$L_2(t, \tau) = \frac{d}{dt} \left\{ \frac{t-\tau}{\bar{t}-\bar{\tau}} \right\} = \frac{1}{\bar{t}-\bar{\tau}} - \frac{t-\tau}{(\bar{t}-\bar{\tau})^2} \frac{d\bar{t}}{dt} \tag{4}$$

In Eq. (1), both “ τ ” and “ t_o ” are located on the boundary Γ , and the increase “ $d\bar{t}$ ” is adopted along the boundary Γ in the anti-clockwise direction (Fig. 1). In Eq. (2), $Q(t) = \sigma_N(t) + i\sigma_{NT}(t)$ denotes

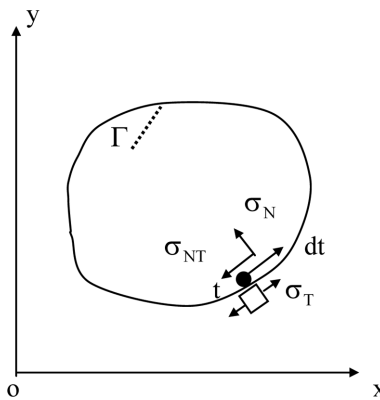


Fig. 1 Formulation of BIE for an exterior region

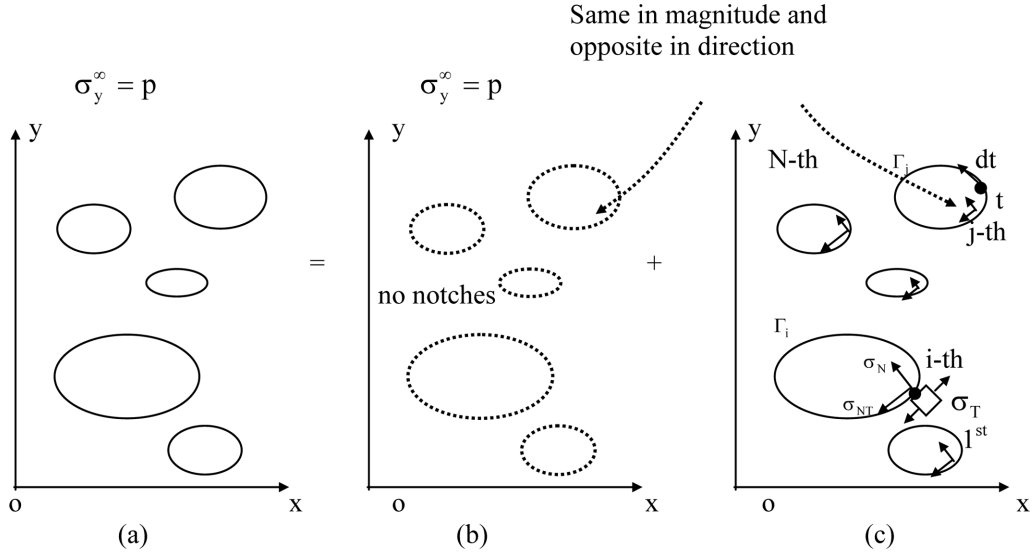


Fig. 2 Formulation of multiple notch problem: (a) the original problem, (b) the uniform stress field and (c) the perturbation field

the traction applied on the boundary and $U(t) = u(t) + iv(t)$ denotes the boundary displacements. In Eq. (3) G denotes the shear modulus of elasticity, $\kappa = 3 - 4\nu$ in plane strain case, and ν the Poisson's ratio. B_1 and B_2 are two elastic constants.

It is assumed that the remote loading is $\sigma_y^\infty = p$, and many elliptic notches are placed in an infinite plate (Fig. 2). The proposed original problem shown by Fig. 2(a) can be considered as a superposition of two problems shown by Fig. 2(b) and (c) respectively. The stress distribution for the uniform field shown by Fig. 2(b) is easy to find out. In the problem shown by Fig. 2(c), the applied loadings on the contours are same in magnitude and opposite in direction to those in the uniform field shown by Fig. 2(b). Therefore, the aim of this study is to solve the boundary value problem (BVP) shown by Fig. 2(c) numerically.

For the multiple notch problem shown by Fig. 2(c), Eq. (1) can be rewritten as

$$\begin{aligned}
 & \frac{U(t_o)}{2} - B_1 i \int_{\Gamma_i} \left(\frac{\kappa - 1}{t - t_o} U(t) dt - L_1(t, t_o) U(t) dt + L_2(t, t_o) \overline{U(t)} dt \right) \\
 & = -B_2 i \int_{\Gamma_i} \left(2\kappa \ln|t - t_o| Q(t) dt + \frac{t - t_o}{\bar{t} - \bar{t}_o} \overline{Q(t)} d\bar{t} \right) \\
 & + B_1 i \sum_{j=1}^N{}' \int_{\Gamma_j} \left(\frac{\kappa - 1}{t - t_o} U(t) dt - L_1(t, t_o) U(t) dt + L_2(t, t_o) \overline{U(t)} dt \right) \\
 & - B_2 i \sum_{j=1}^N{}' \int_{\Gamma_j} \left(2\kappa \ln|t - t_o| Q(t) dt + \frac{t - t_o}{\bar{t} - \bar{t}_o} \overline{Q(t)} d\bar{t} \right) \quad (t_o \in \Gamma_i, i = 1, 2, \dots, N) \quad (5)
 \end{aligned}$$

where $\sum_{j=1}^N{}'$ means that the term $j = i$ should be excluded in the summation.

A particular feature of Eq. (5) is as follows. If $t_o \in \Gamma_i$ and the integration “ dt ” is performed along the boundary Γ_j with $i \neq j$, the relevant kernels in Eq. (5) are not singular.

2.2 Discretization of the BIE and the iteration method

After discretization, Eq. (5) may be written as follows

$$[\mathbf{G}_i]\{u_i\} = [\mathbf{H}_i]\{q_i\} - \sum_{j=1}^N ' [\mathbf{G}_{ij}]\{u_j\} + \sum_{j=1}^N ' [\mathbf{H}_{ij}]\{q_j\}, \quad (i = 1, 2, \dots, N) \tag{6}$$

where $\sum_{j=1}^N '$ means that the term $j = i$ should be excluded in the summation. Note that, the vector $\{u_i\}$ is composed of many (u, v) components at many discrete points along the boundary, and the vector $\{q_i\}$ is composed of many (σ_N, σ_{NT}) components at many discrete points along the boundary Γ_i .

Note that, the vectors $\{q_i\} = \{\tilde{q}_i\}$ ($i = 1, 2, \dots, N$) are given beforehand. Thus, Eq. (6) can be rewritten as

$$[\mathbf{G}_i]\{u_i\} = [\mathbf{H}_i]\{\tilde{q}_i\} - \sum_{j=1}^N ' [\mathbf{G}_{ij}]\{u_j\} + \sum_{j=1}^N ' [\mathbf{H}_{ij}]\{\tilde{q}_j\}, \quad (i = 1, 2, \dots, N) \tag{7}$$

Physically, $[\mathbf{G}_{ij}]$ represents a matrix acting upon displacement where the field point t_o is on the i -th notch and the source point “ p ” and “ d ” are on the j -th notch

Since the matrix $[\mathbf{G}_i]$ is invertible (Chen *et al.* 2009). Thus, from Eq. (7) we have

$$\{u_i\} = - \sum_{j=1}^N ' [\mathbf{C}_{ij}]\{u_j\} + \{\tilde{p}_i\}, \quad (i = 1, 2, \dots, N) \tag{8}$$

where

$$[\mathbf{C}_{ij}] = [\mathbf{G}_i^{-1}][\mathbf{G}_{ij}], \quad \{\tilde{p}_i\} = [\mathbf{B}_i]\{\tilde{q}_i\} + \sum_{j=1}^N ' [\mathbf{D}_{ij}]\{\tilde{q}_j\}$$

$$[\mathbf{B}_i] = [\mathbf{G}_i^{-1}][\mathbf{H}_i], \quad [\mathbf{D}_{ij}] = [\mathbf{G}_i^{-1}][\mathbf{H}_{ij}] \tag{9}$$

For the algebraic Eq. (8), we propose the following iteration

$$\{u_i^{(m+1)}\} = - \sum_{j=1}^N ' [\mathbf{C}_{ij}]\{u_j^{(m)}\} + \{\tilde{p}_i\}, \quad (i = 1, 2, \dots, N) \tag{10}$$

In computation, we may assume $\{u_j^{(1)}\} = \{0\}$. From Eq. (10), we can get $\{u_j^{(m)}\}$ ($m = 2, 3, \dots$) successfully.

Sometimes, one may propose an alternative scheme for iteration as follows

$$\{u_i^{(m+1)}\} = \alpha \{u_i^{(m)}\} + (1 - \alpha) \left[- \sum_{j=1}^N ' [\mathbf{C}_{ij}]\{u_j^{(m)}\} + \{\tilde{p}_i\} \right], \quad (i = 1, 2, \dots, N) \tag{11}$$

It is seen that, if $\alpha = 0$, Eq. (11) will be reduced to Eq. (10). It is proved that in the following numerical examples that all iterations are convergent if $\alpha = 0.25$ is adopted.

In fact, in some simple cases, for examples, in the case of two notches, there is no need to use the

alternative scheme of iteration. However, in the case of five notches, particularly, in the case of narrow spacing between notches, the suggested alternative scheme is necessary in computation. The parameter α is simply determined by some test computation. It is known that, once a FORTRAN program is composed, it is an easy task for changing the parameter from $\alpha = 0.1$ to $\alpha = 0.2, \dots$, which needs a few minutes.

The iteration is completed under the following condition is satisfied

$$\max\{|u_j^{(m+1)}\} - \{u_j^{(m)}\}| < \{\varepsilon\} \quad (\text{where } \varepsilon \text{ a small value}) \quad (12)$$

After the vectors $\{u_i\}$ ($i = 1, 2, \dots, N$) are obtained, the hoop stress σ_T can be evaluated immediately (Figs. 1, 2). To this end, the following technique is suggested. In fact, in the plane strain case, the strain component ε_T (in T -direction) can be expressed by using Hook's law

$$\varepsilon_T = \frac{1}{E}(\sigma_T(1 - \nu^2) - \nu(1 + \nu)\sigma_N) \quad (13)$$

or

$$\sigma_T = \frac{E\varepsilon_T + \nu(1 + \nu)\sigma_N}{1 - \nu^2} \quad (14)$$

where E is the Young's modulus of elasticity. In Eq. (14), the component σ_N is from input datum, and ε_T is the strain in the T -direction which can be evaluated from the solution of displacements on the boundary. Thus, the value of σ_T at discrete points is obtainable.

3. Numerical examples

Several numerical examples are provided to prove the efficiency of the suggested method. In the examples, the plane strain condition and $\nu = 0.3$ are assumed. In computation, we choose $\varepsilon = 10^{-5}$ for the error tolerance in Eq. (12). It is proved in the following numerical examples that all iterations in Eq. (11) are convergent if $\alpha = 0.25$ is adopted. Stress concentration factors (SIFs) are evaluated in all examples.

As claimed previously, the original field for the notch problem is a superposition of the uniform field and a perturbation field, which is shown in Fig. 2. In all following examples below, the stress contribution from the uniform field has been added to the final result.

Example 1

The first example is devoted to examine the achieved accuracy for the suggested method (Fig. 3(a)). In the example, we assume that two elliptic notches are in series. The elliptic notch has the half-axis " a " and " b " and the spacing between two notches is denoted by " c ". The remote loading is denoted by $\sigma_y^\infty = p$. In the solution of BIE, 96 divisions are used for the discretization of elliptic contour.

It is known that for the single notch case, the maximum hoop stress at the crown point is $p_c = (1 + 2a/b)p$. For the following cases: $b/a = 0.25, 1/3, 0.5$ and 1.0 and $c/a = 0.1, 0.2, \dots$ to 1.0 , the hoop stresses at the point " E " and " G " are denoted by

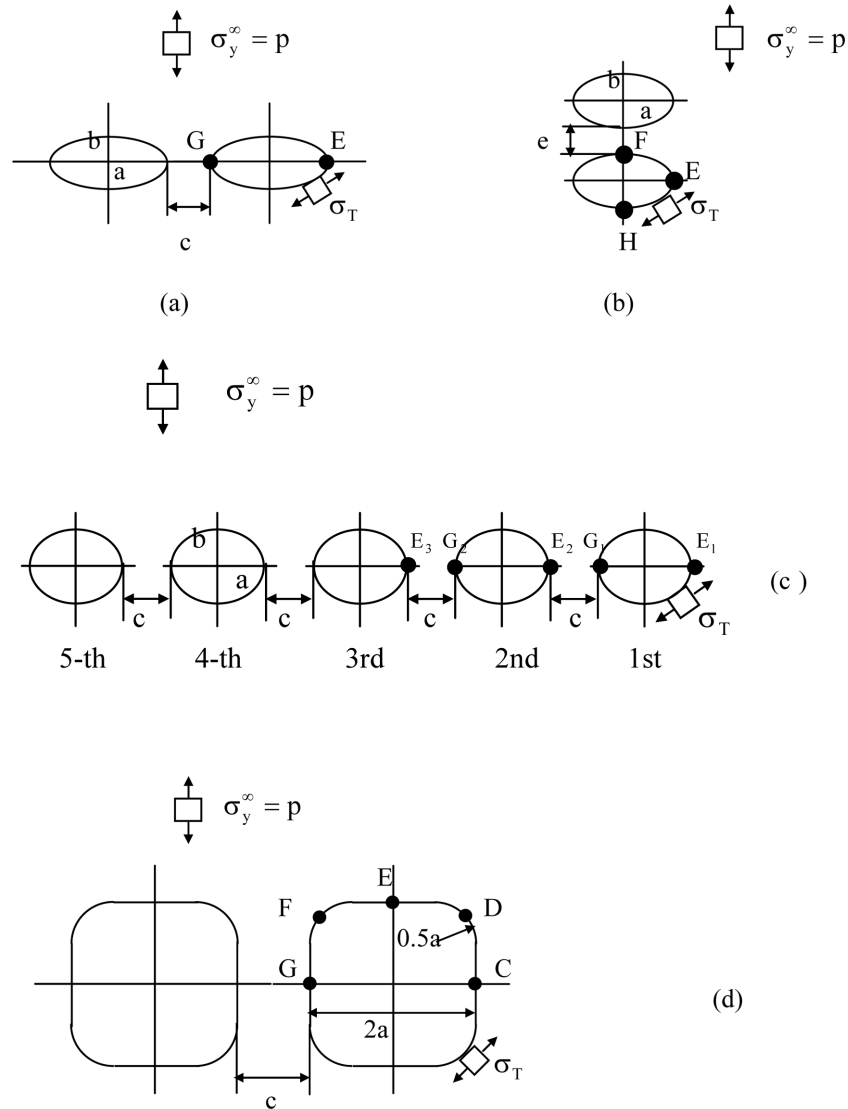


Fig. 3 (a) two elliptic holes in series under remote tension $\sigma_y^\infty = p$, (b) two elliptic holes in a stacking position under remote tension $\sigma_y^\infty = p$, (c) five elliptic holes in series under remote tension $\sigma_y^\infty = p$, (d) two square holes with round corners in series under remote tension $\sigma_y^\infty = p$

$$\sigma_{T,E} = s_E(b/a, c/a)p_c, \quad \sigma_{T,G} = s_G(b/a, c/a)p_c, \quad \text{with} \quad p_c = \left(1 + \frac{2a}{b}\right)p \quad (15a)$$

The computed non-dimensional stress concentration factors $s_E(b/a, c/a)$ and $s_G(b/a, c/a)$ are listed in Table 1. It is found that in the case of $b/a = 0.25$ and $c/a = 0.1$, or a rather narrow spacing case, the stress concentration factor can reach a huge value, or $\sigma_{T,G} = 1.915p_c = 17.235p$ ($p_c = 9p$ in the case of $b/a = 0.25$). In addition, for the case of $b/a = 1/3$, the computed results coincide with those obtained by other researcher (Tsukrov and Kachanov 1997).

Table 1 Non-dimensional stress concentration factors $s_E(b/a, c/a)$ (at the point E) and $s_G(b/a, c/a)$ (at the point G) for two elliptic notches in series under the remote loading $\sigma_y^\infty = p$, with $s = \sigma_T/p_c$, $p_c = (1 + (2a/b))p$ (see Fig. 3(a) and Eq. (15a))

$s_E(b/a, c/a)$										
$c/a =$	0.1	0.2	0.3	0.4	0.5	0.6	0.7	0.8	0.9	1.0
$b/a =$										
0.25	1.153	1.120	1.101	1.087	1.077	1.069	1.062	1.057	1.052	1.048
1/3	1.156	1.121	1.101	1.087	1.076	1.068	1.061	1.055	1.051	1.047
1/3*	1.150	1.120	1.090	1.080	1.070	1.065	1.060	1.050	1.045	1.040
0.50	1.163	1.126	1.104	1.089	1.078	1.068	1.061	1.055	1.050	1.046
0.75	1.169	1.133	1.111	1.095	1.082	1.073	1.065	1.058	1.052	1.047
1.00	1.172	1.138	1.116	1.100	1.087	1.077	1.069	1.062	1.056	1.050
$s_G(b/a, c/a)$										
$c/a =$	0.1	0.2	0.3	0.4	0.5	0.6	0.7	0.8	0.9	1.0
$b/a =$										
0.25	1.915	1.485	1.331	1.250	1.200	1.165	1.141	1.122	1.107	1.095
1/3	2.053	1.527	1.342	1.249	1.194	1.158	1.132	1.113	1.098	1.087
1/3*	2.060	1.510	1.330	1.240	1.180	1.150	1.130	1.110	1.090	1.080
0.50	2.338	1.658	1.405	1.278	1.205	1.158	1.126	1.104	1.088	1.075
0.75	2.658	1.867	1.545	1.371	1.265	1.195	1.148	1.115	1.091	1.073
1.00	2.860	2.028	1.675	1.475	1.346	1.259	1.196	1.151	1.117	1.091

*from (Tsukrov and Kachanov 1997).

Table 2 Non-dimensional stress concentration factors $h_E(b/a, c/a)$ (at the point E) and $h_G(b/a, c/a)$ (at the point G) for two elliptic notches in series under the remote loading $\sigma_y^\infty = p$ (see Fig. 3(a) and Eq. (15b))

$h_E(b/a, c/a)$										
$c/a =$	0.1	0.2	0.3	0.4	0.5	0.6	0.7	0.8	0.9	1.0
$b/a =$										
0.2	12.675	12.323	12.115	11.970	11.859	11.772	11.700	11.640	11.589	11.544
0.2*	NA									
$h_G(b/a, c/a)$										
$c/a =$	0.1	0.2	0.3	0.4	0.5	0.6	0.7	0.8	0.9	1.0
$b/a =$										
0.2	20.339	16.203	14.645	13.801	13.265	12.891	12.616	12.404	12.236	12.100
0.2*	20.3	16.3	14.9	14.0	13.8	13.0	12.9	12.8	12.7	12.5

*measured from a figure in Ting *et al.* (1999)

NA not available

In addition, other comparison with the method developed by Ting *et al.* (1999c) is carried out. Alternatively, the computed results are expressed as

$$\sigma_{T,E} = h_E(b/a, c/a)p, \quad \sigma_{T,G} = h_G(b/a, c/a)p \tag{15b}$$

In the case of $b/a = 0.2$ and $c/a = 0.1, 0.2, \dots$ to 1.0 , the computed results are listed in Table 2. From tabulated results we see that the deviation from different methods is minor.

Example 2

In the second example, two elliptic notches are in a stacking position (Fig. 3(b)). The same computation conditions used in Example 1 are used in this example.

For the following cases: $b/a = 0.25, 0.5, 0.75$ and 1.0 and $e/b = 0.2, 0.4, \dots$ to 2.0 , the hoop stresses at the point “E” “F” and “H” are denoted by

$$\sigma_{T,E} = s_E(b/a, e/b)p, \quad \sigma_{T,F} = s_F(b/a, e/b)p, \quad \sigma_{T,H} = s_H(b/a, e/b)p \tag{16}$$

The computed non-dimensional stress concentration factors $s_E(b/a, e/b)$, $s_F(b/a, e/b)$ and $s_H(b/a, e/b)$ are listed in Table 3.

Table 3 Non-dimensional stress concentration factors $s_E(b/a, c/a)$ (at the point E), and $s_F(b/a, c/a)$ (at the point F), and $s_H(b/a, c/a)$ (at the point H) for two elliptic notches in stacking position under the remote loading $\sigma_y^\infty = p$ (see Fig. 3(b) and Eq. (16))

$s_E(b/a, c/a)$										
$e/b =$	0.2	0.4	0.6	0.8	1.0	1.2	1.4	1.6	1.8	2.0
$b/a =$										
0.25	7.080	7.321	7.558	7.784	7.986	8.156	8.295	8.407	8.497	8.570
0.50	4.194	4.394	4.561	4.679	4.759	4.814	4.853	4.881	4.902	4.918
0.75	3.207	3.367	3.470	3.531	3.568	3.592	3.608	3.620	3.628	3.634
1.00	2.701	2.824	2.890	2.926	2.947	2.960	2.969	2.975	2.979	2.983
$s_F(b/a, c/a)$										
$e/b =$	0.2	0.4	0.6	0.8	1.0	1.2	1.4	1.6	1.8	2.0
$b/a =$										
0.25	-0.384	-0.320	-0.444	-0.579	-0.682	-0.756	-0.808	-0.846	-0.874	-0.895
0.50	-0.342	-0.589	-0.753	-0.839	-0.887	-0.916	-0.935	-0.948	-0.957	-0.963
0.75	-0.482	-0.751	-0.860	-0.910	-0.936	-0.952	-0.961	-0.968	-0.972	-0.976
1.00	-0.605	-0.829	-0.905	-0.937	-0.954	-0.964	-0.970	-0.974	-0.977	-0.979
$s_H(b/a, c/a)$										
$e/b =$	0.2	0.4	0.6	0.8	1.0	1.2	1.4	1.6	1.8	2.0
$b/a =$										
0.25	-0.867	-0.855	-0.862	-0.875	-0.889	-0.903	-0.915	-0.926	-0.934	-0.942
0.50	-0.869	-0.885	-0.908	-0.927	-0.941	-0.952	-0.959	-0.965	-0.969	-0.973
0.75	-0.883	-0.912	-0.935	-0.950	-0.960	-0.967	-0.972	-0.975	-0.978	-0.980
1.00	-0.897	-0.929	-0.949	-0.960	-0.968	-0.973	-0.976	-0.978	-0.980	-0.981

It is found that in the case of a rather narrow spacing between notches, the stacking effect is rather higher. For example, in the case of $b/a = 0.25$ and $e/b = 0.2$, we have $s_E(b/a, e/b) = 7.080$ and $s_F(b/a, e/b) = -0384$. However, in a single notch of $b/a = 0.25$, we have $s_E = 9.000$ and $s_F = -1.000$.

Example 3

In the third example, we assume that five elliptic notches are in series. The elliptic notch has the half-axis “ a ” and “ b ” and the spacing between two notches is denoted by “ c ” (Fig. 3(c)). The remote loading is denoted by $\sigma_y^\infty = p$. In the solution of BIE, 96 divisions are used for the discretization of elliptic contour.

For the following cases: $b/a = 0.25, 0.5, 0.75$ and 1.0 and $c/a = 0.1, 0.2, \dots$ to 1.0 , the hoop stresses at the points “ E_j ”, “ G_j ” ($j = 1, 2, 3$) are denoted by (see Fig. 3(c))

$$\begin{aligned} \sigma_{T,E_1} &= s_{E_1}(b/a, c/a)p, & \sigma_{T,G_1} &= s_{G_1}(b/a, c/a)p & \text{(for the first notch)} \\ \sigma_{T,E_2} &= s_{E_2}(b/a, c/a)p, & \sigma_{T,G_2} &= s_{G_2}(b/a, c/a)p & \text{(for the second notch)} \\ \sigma_{T,E_3} &= s_{E_3}(b/a, c/a)p & & & \text{(for the third notch)} \end{aligned} \tag{17}$$

The computed non-dimensional stress concentration factors $s_{E_1}(b/a, c/a), s_{G_1}(b/a, c/a), s_{E_2}(b/a, c/a), s_{G_2}(b/a, c/a)$ and $s_{E_3}(b/a, c/a)$ are listed in Table 4. It is found that in the case of $b/a = 0.25$ and $c/a = 0.1$, or a rather narrow spacing case, the stress concentration factor can reach a huge value, for example, we have $s_{E_1}(b/a, c/a) = 11.584, s_{G_1}(b/a, c/a) = 20.947, s_{E_2}(b/a, c/a) = 21.553, s_{G_2}(b/a, c/a) = 23.186$ and $s_{E_3}(b/a, c/a) = 23.317$, respectively. We see from listed results that the central notch is under most severe loading condition. We know that, in a single notch with the ratio $b/a = 0.25$, the non-dimensional stress concentration factor is $s_F = (1 + 2a/b)_{a/b=4} = 9$.

Table 4 Non-dimensional stress concentration factors $s_{E_1}(b/a, c/a)$ (at the point E_1), $s_{G_1}(b/a, c/a)$ (at the point G_1), $s_{E_2}(b/a, c/a)$ (at the point E_2), $s_{G_2}(b/a, c/a)$ (at the point G_2), $s_{E_3}(b/a, c/a)$ (at the point E_3) for five elliptic notches in series position under the remote loading $\sigma_y^\infty = p$ (see Fig. 3(c) and Eq. (17))

$s_{E_1}(b/a, c/a)$										
$c/a =$	0.1	0.2	0.3	0.4	0.5	0.6	0.7	0.8	0.9	1.0
$b/a =$										
0.25	11.584	10.917	10.558	10.319	10.145	10.011	9.904	9.816	9.743	9.680
0.50	6.605	6.162	5.924	5.768	5.656	5.570	5.503	5.448	5.403	5.365
0.75	4.952	4.602	4.410	4.282	4.190	4.119	4.063	4.018	3.980	3.948
1.00	4.112	3.821	3.657	3.546	3.465	3.403	3.353	3.313	3.279	3.250
$s_{G_1}(b/a, c/a)$										
$c/a =$	0.1	0.2	0.3	0.4	0.5	0.6	0.7	0.8	0.9	1.0
$b/a =$										
0.25	20.947	15.319	13.297	12.239	11.583	11.135	10.809	10.562	10.368	10.212
0.50	14.737	9.739	7.935	7.037	6.515	6.182	5.954	5.791	5.669	5.576
0.75	12.675	8.238	6.524	5.623	5.081	4.730	4.490	4.320	4.195	4.101
1.00	11.429	7.472	5.888	5.024	4.484	4.121	3.865	3.678	3.539	3.434

Table 4 Continued

$s_{E_2}(b/a, c/a)$										
$c/a =$	0.1	0.2	0.3	0.4	0.5	0.6	0.7	0.8	0.9	1.0
$b/a =$										
0.25	21.553	15.896	13.833	12.735	12.042	11.561	11.205	10.931	10.713	10.535
0.50	15.136	10.116	8.278	7.348	6.798	6.439	6.190	6.008	5.870	5.761
0.75	12.980	8.546	6.809	5.883	5.317	4.944	4.685	4.498	4.358	4.251
1.00	11.651	7.731	6.138	5.257	4.698	4.316	4.043	3.842	3.689	3.571
$s_{G_2}(b/a, c/a)$										
$c/a =$	0.1	0.2	0.3	0.4	0.5	0.6	0.7	0.8	0.9	1.0
$b/a =$										
0.25	23.186	16.688	14.331	13.084	12.302	11.763	11.367	11.063	10.822	10.627
0.50	16.478	10.705	8.621	7.574	6.959	6.559	6.283	6.081	5.929	5.810
0.75	14.262	9.117	7.138	6.095	5.464	5.051	4.766	4.560	4.407	4.291
1.00	12.893	8.302	6.472	5.474	4.849	4.425	4.125	3.904	3.738	3.611
$s_{E_3}(b/a, c/a)$										
$c/a =$	0.1	0.2	0.3	0.4	0.5	0.6	0.7	0.8	0.9	1.0
$b/a =$										
0.25	23.317	16.807	14.439	13.181	12.390	11.843	11.440	11.130	10.885	10.685
0.50	16.567	10.786	8.692	7.637	7.014	6.609	6.328	6.122	5.966	5.844
0.75	14.332	9.185	7.198	6.148	5.511	5.093	4.803	4.594	4.438	4.319
1.00	12.945	8.360	6.526	5.523	4.893	4.465	4.160	3.936	3.767	3.637

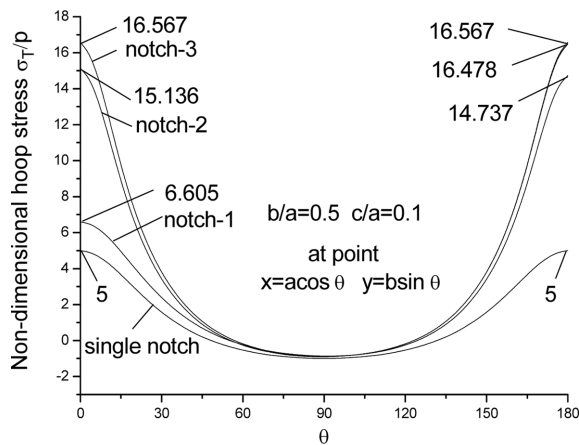


Fig. 4 The hoop stress distributions $\sigma_T = p$ along the contours of first, second and third notch in the case of $b/a = 0.5$ and $c/a = 0.1$ (see Fig. 3(c))

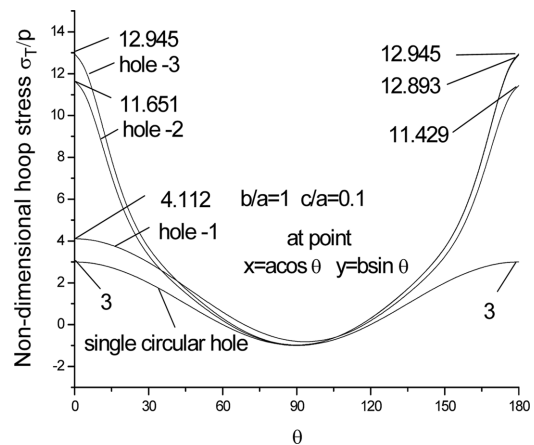


Fig. 5 The hoop stress distributions $\sigma_T = p$ along the contours of first, second and third notch in the case of $b/a = 1$ and $c/a = 0.1$ (see Fig. 3(c))

Table 5 Non-dimensional stress concentration factors $s_C(c/a), s_D(c/a), s_E(c/a), s_F(c/a)$ and $s_G(c/a)$ for two square notches in series position under the remote loading $\sigma_y^\infty = p$ (see Fig. 3(d) and Eq. (18))

$c/a =$	0.1	0.2	0.3	0.4	0.5	0.6	0.7	0.8	0.0	1.0
Points										
C	2.233	2.171	2.128	2.096	2.070	2.049	2.031	2.016	2.003	1.992
D	2.138	2.032	1.960	1.906	1.864	1.830	1.802	1.778	1.757	1.740
E	-0.826	-0.817	-0.810	-0.804	-0.799	-0.795	-0.791	-0.788	-0.786	-0.783
F	1.284	1.723	1.908	1.993	2.033	2.049	2.053	2.049	2.042	2.031
G	5.424	4.340	3.740	3.341	3.045	2.812	2.625	2.474	2.352	2.254

For two cases (a) $b/a = 0.5$ and $c/a = 0.1$ and (b) $b/a = 1$ and $c/a = 0.1$, the non-dimensional $s = \sigma_T/p$ along the three notch contours are plotted in Figs. 4 and 5, respectively. From Figs. 4 and 5 we see that the central notch is under most severe loading condition.

As claimed above, for the case of five notches, the suggested alternative scheme of iteration shown by Eq. (11) is necessary in computation. For a narrow spacing case, for example, in $b/a = 0.5$ and $c/a = 0.1$, the number of iteration is 38. However, in the wider spacing case, for example, in $b/a = 0.5$ and $c/a = 1$, the number of iteration is reduced to 15.

Example 4

The fourth example is devoted to find out SCFs for two square notches with the round corners (Fig. 3(d)). The square notch has a width “ $2a$ ”, and the corner has a radius “ $0.5a$ ”. The spacing between two notches is denoted by “ c ”. The remote loading is denoted by $\sigma_y^\infty = p$. In the solution of BIE, 96 divisions are used for the discretization of contour.

In the case of and $c/a = 0.1, 0.2, \dots$ to 1.0, the hoop stresses at the point “C”, “D” “E” “F” and “G” points of the left notch are denoted by

$$\begin{aligned} \sigma_{T,C} &= s_C(c/a)p, & \sigma_{T,D} &= s_D(c/a)p, & \sigma_{T,E} &= s_E(c/a)p \\ \sigma_{T,F} &= s_F(c/a)p, & \sigma_{T,G} &= s_G(c/a)p \end{aligned} \quad (18)$$

The computed non-dimensional stress concentration factors $s_C(c/a), s_D(c/a), s_E(c/a), s_F(c/a)$ and $s_G(c/a)$ are listed in Table 5. It is found that in the case of $c/a = 0.1$, or a rather narrow spacing case, the stress concentration factor at the point “G” can reach a large value, or $s_G(c/a)|_{c/a=0.1} = 5.422$. However, at the opposite point “C”, SCF has a smaller value $s_C(c/a)|_{c/a=0.1} = 2.233$.

4. Conclusions

Some advantages can be found from the suggested formulation. It is assumed that the problem for five notches will be solved, and 96 divisions along the boundary are used in computation. In the case, for example, the matrices $[G_i]$ ($i = 1, 2..5$) have a dimension (192*192). If we do not use the iteration method, and use Eq. (8) to solve the problem directly, we need to formulate $[G_1], [G_{12}], [G_{13}], [G_{14}], [G_{15}], \dots$ total 25 matrices. In addition, one needs to assemble those matrices in a larger matrix, which has a dimension (960*960). In fact, it is a rather complicated work to assemble so many matrices in a larger matrix. This is an inconvenient point in the direct solution from

Eq. (8). In the meantime, if we use iteration shown by Eqs. (10) or (11) to solve the problem, we do not need to assemble many matrices in a proper position of a larger matrix. In real computation, the iteration needs a short time on a personal computer. Particularly, we have examined that the 40 sets of solution (or $b/a = 0.25, 0.5, 0.75$ and 1 , $c/a = 0.1, 0.2, \dots$) for five notches in Example 3 only took 3 minutes and 55 seconds by using a FORTRAN program.

Secondly, the suggested method can be used to arbitrary shapes for the contours. For example, we have solved the problem for two square notches with round corners in the fourth example. Thirdly, the suggested iteration method based on BIE can provide accurate results for stress concentration factors, which was shown in the first example.

As stated above, a boundary element method was developed to analyze the stress concentration problems of multiple elliptical holes in an infinite domain (Ting *et al.* 1999c). In the formulation, the tractions on the hole contours were chosen as an iteration parameter. In fact, the formulation is based on the superposition method (Ting *et al.* 1999). On the other hand, the displacements on the contours are chosen as an iteration parameter in this paper. Secondly, the BIE is formulated on the boundary of notches, and no superposition method is used in the formulation.

References

- Brebbia, C.A., Telles, J.C.F. and Wrobel, L.C. (1984), *Boundary Element Techniques - Theory and Applications in Engineering*, Springer, Heidelberg.
- Chen, J.T., Liang, M.T. and Yang, S.S. (1995), "Dual boundary integral equations for exterior problems", *Eng. Anal. Boun. Elem.*, **16**, 333-340.
- Chen, J.T. and Chen, Y.W. (2000), "Dual boundary element analysis using complex variables for potential problems with or without a degenerate boundary", *Eng. Anal. Boun. Elem.*, **24**, 671-684.
- Chen, J.T., Kuo, S.R. and Lin, J.H. (2002), "Analytical study and numerical experiments for degenerate scale problems in the boundary element method for two-dimensional elasticity", *Int. J. Numer. Meth. Eng.*, **54**, 1669-1681.
- Chen, J.T. and Wu, A.C. (2007), "Null-field approach for the multi-inclusion problem under antiplane shears", *J. Appl. Mech.*, **74**, 469-487.
- Chen, J.T. and Lee, Y.T. (2009), "Torsional rigidity of a circular bar with multiple circular inclusions using the null-field integral approach", *Comput. Mech.*, **44**, 221-232.
- Chen, Y.Z., Wang, Z.X. and Lin, X.Y. (2009), "A new kernel in BIE and the exterior boundary value problem in plane elasticity", *Acta Mech.*, **206**, 207-224.
- Chen, Y.Z. and Lin, X.Y. (2010), "Dual boundary integral equation formulation in plane elasticity using complex variable", *Eng. Anal. Boun. Elem.*, **34**, 834-844.
- Chen, Y.Z. (2011), "Solution of periodic notch problems in an infinite plate using BIE in conjunction with remainder estimation technique", *Struct. Eng. Mech.*, **38**, 619-631.
- Cheng, A.H.D. and Cheng, D.S. (2005), "Heritage and early history of the boundary element method", *Eng. Anal. Boun. Elem.*, **29**, 286-302.
- Cruse, T.A. (1969), "Numerical solutions in three-dimensional elastostatics", *Int. J. Solids Struct.*, **5**, 1259-1274.
- Denda, M. and Kosaka, I. (1997), "Dislocation and point-force-based approach to the special Green's function BEM for elliptic hole and crack problems in two dimensions", *Int. J. Numer. Meth. Eng.*, **40**, 2857-2889.
- Dong, C.Y. and Lee, K.Y. (2006), "Boundary element implementation of doubly periodic inclusion problems", *Eng. Anal. Boun. Elem.*, **30**, 662-670.
- Dong, C.Y. (2006), "Effective elastic properties of doubly periodic array of inclusions of various shapes by the boundary element method", *Int. J. Solids Struct.*, **43**, 7919-7938.
- Hong, H.K. and Chen, J.T. (1988), "Derivations of integral equations of elasticity", *J. Eng. Mech.*, **114**, 1028-1044.

- Isida, M. and Igawa, H. (1991), "Analysis of a zig-zag array of circular holes in an infinite solid under uniaxial tension", *Int. J. Solids Struct.*, **27**, 849-864.
- Jaswon, M.A. and Symm, G.T. (1967), *Integral Equation Methods in Potential Theory and Elastostatics*, Academic Press, London.
- Kolte, R., Ye, W., Hui, C.Y. and Mukherjee, S. (1996), "Complex variable formulations for usual and hypersingular integral equations for potential problems—with applications to corners and cracks", *Comput. Mech.*, **17**, 279-286.
- Linkov, A.M. (2002), *Boundary Integral Equations in Elasticity*, Kluwer, Dordrecht.
- Nisitani, H. (1978), "Solutions of notch problems by body force method", *Mechanics of Fracture*, Vol. 5, Stress Analysis of Notch Problems, Ed. G.C. Sih, Noordhoff, Netherlands.
- Mogilevskaya, S.G. and Linkov, A.M. (1998), "Complex fundamental solutions and complex variables boundary element method in elasticity", *Comput. Mech.*, **22**, 88-92.
- Mogilevskaya, S.G. (2000), "Complex hypersingular integral equation for the piecewise homogeneous half-plane with cracks", *Int. J. Fract.*, **102**, 177-204.
- Muskhelishvili, N.I. (1963), *Some Basic Problems of the Mathematical Theory of Elasticity*, Noordhoff, Groningen.
- Rizzo, F.J. (1967), "An integral equation approach to boundary value problems in classical elastostatics", *Quart. J. Appl. Math.*, **25**, 83-95.
- Savin, G.N. (1961), *Stress Concentration Around Holes*, Pergamon Press, New York.
- She, C.M. and Guo, W.L. (2007), "Three-dimensional stress concentrations at elliptic holes in elastic isotropic plates subjected to tensile stress", *Int. J. Fatigue*, **29**, 330-335.
- She, C.M., Zhao, J.H. and Guo, W.L. (2008), "Three-dimensional stress fields near notches and cracks", *Int. J. Fract.*, **151**, 151-160.
- Ting, K., Chen, K.T. and Yang, W.S. (1999a), "Applied alternating method to analyze the stress concentration around interacting multiple circular holes in an infinite domain", *Int. J. Solids Struct.*, **36**, 533-556.
- Ting, K., Chen, K.T. and Yang, W.S. (1999b), "Stress analysis of the multiple circular holes with the rhombic array using alternating method", *Int. J. Pres. Ves. Pip.*, **76**, 503-514.
- Ting, K., Chen, K.T. and Yang, W.S. (1999c), "Boundary element method applied to analyze the stress concentration problems of multiple elliptical holes in an infinite domain", *Nucl. Eng. Des.*, **187**, 303-313.
- Tsukrov, I. and Kachanov, M. (1997), "Stress concentrations and microfracturing patterns in a brittle-elastic solid with interacting pores of diverse shapes", *Int. J. Solids Struct.*, **34**, 2887-2904.
- Wang, J.L., Crouch, S.L. and Mogilevskaya, S.G. (2003), "A complex boundary integral for multiple circular holes in an infinite plane", *Eng. Anal. Boun. Elem.*, **27**, 789-802.
- Yang, Z. (2009), "The stress and strain concentrations of an elliptical hole in an elastic plate of finite thickness subjected to tensile stress", *Int. J. Fract.*, **155**, 43-54.
- Yang, Z., Kim, C.B., Cho, C. and Beom, H.G. (2008), "The concentration of stress and strain in finite thickness elastic plate containing a circular hole", *Int. J. Solids Struct.*, **45**, 713-731.
- Zhang, X.S. and Zhang, X.X. (2008), "Exact integration for hypersingular boundary integral equation of two-dimensional elastostatics", *Struct. Eng. Mech.*, **30**, 279-296.